THE JOURNAL OF PHYSICAL CHEMISTRY B

Article

pubs.acs.org/JPCB

Toward an Accurate Conformational Modeling of Iduronic Acid

Pavel Oborský,[†] Igor Tvaroška,[‡] Blanka Králová,[†] and Vojtěch Spiwok*[,†,‡]

[†]Department of Biochemistry and Microbiology, Institute of Chemical Technology, Prague, Technická 3, Prague 6 166 28, Czech Republic

[‡]Department of Structure and Function of Saccharides, Institute of Chemistry, Center for Glycomics, Slovak Academy of Sciences, Dúbravská cesta 9, 845 38 Bratislava, Slovak Republic

Supporting Information

ABSTRACT: Iduronic acid (IdoA), unlike most other monosaccharides, can adopt different ring conformations, depending on the context of the molecular structure. Accurate modeling of this building block is essential for understanding the role of glycosaminoglycans and other glycoconjugates. Here, we use metadynamics to predict equilibria of $^{1}C_{4}$, $^{4}C_{1}$ and $^{2}S_{O}$ conformations of α-L-IdoA-OMe and α-L-IdoA2S-OMe. Different schemes of scaling of atoms separated by three bonds (1−4 interaction) were tested. It was found that scaling (reduction) of 1−4 electrostatic interactions significantly changes conformational preferences toward the $^{4}C_{1}$ conformation. More interestingly, scaling of 1−4 van der Waals interaction favors skew-boat conformations. This shows that a minor modification of noncovalent 1−4 interactions parameters can provide a good agreement between populations of conformers of iduronic acid in water from simulations and experiments.

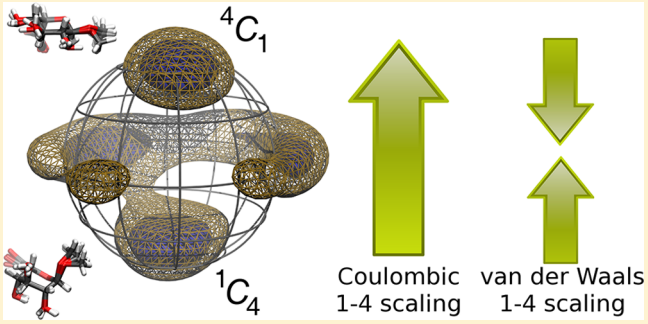

INTRODUCTION

α-L-Iduronic acid (α-L-IdoA, Figure 1) is an essential component of glycosaminoglycans, such as heparins, dermatans, and their sulphates. These polysaccharides play a prominent role in many biological processes, including blood coagulation, cell−cell interactions, angiogenesis, and others.[1] Iduronic acid is an interesting monosaccharide building block for its unique conformational behavior.[2−4] Most monosaccharides prefer a single ring conformation, namely, the chair conformation with the majority of substituents in equatorial positions. Recent studies of common monosaccharides and their derivatives show that other conformations might be populated in water solution at non-negligible and biologically attractive levels.[5−7] High-energy boat and skew boat conformations even become major conformers when the saccharide is bound in the active sites of a carbohydrate-processing enzymes.[8] Some polysaccharides can form boat or skew boat conformations upon mechanical stress.[9] Iduronic acid (IdoA) is perhaps the most biologically interesting monosaccharide that, apart from other common monosaccharide building blocks, exists in solution as an equilibrium mixture of various highly populated conformations ($^{1}C_{4}$, $^{4}C_{1}$ and $^{2}S_{O}$), without any assistance of a protein or mechanical stress. This equilibrium can be perturbed by the context of molecular structure, namely, by neighboring residues, sulphation, and other covalent modifications, as well as by interactions with other molecules.[4,10,11] Accurate modeling of ring puckering and especially modeling of IdoA conformation is, therefore, a challenging task.

The accuracy of prediction of bioactive conformations of molecules by means of molecular modeling depends on the accuracy of the microscopic potential and the effectiveness of sampling. The conformation of IdoA and its derivatives has

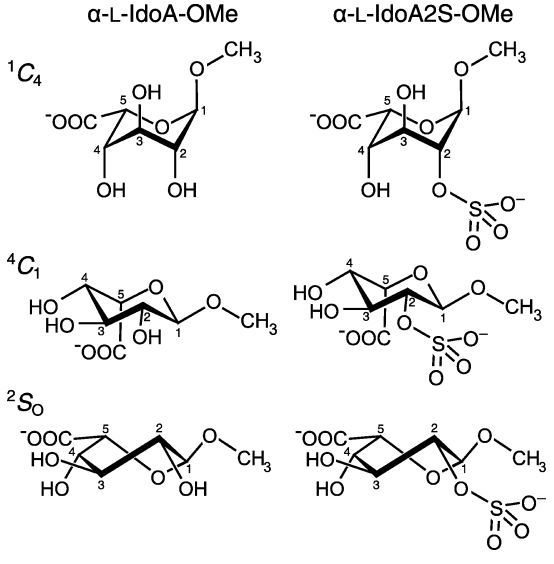

Figure 1. Schematic representation of α-L-IdoA-OMe and α-L-IdoA2S-OMe in $^{4}C_{1}$, $^{1}C_{4}$, and $^{2}S_{O}$ conformations.

Received: October 11, 2012
Revised: December 31, 2012
Published: January 3, 2013

been intensively studied by quantum chemical methods at different levels of theory, in different ionized states and with different counterions or solvation models.[12−18] These methods are in general extremely computationally expensive and do not provide appropriate sampling of different conformations. This can be, at least to a certain extent, achieved by a molecular mechanics potential together with molecular dynamics simulations. However, conformational changes of pyranose rings are rarely occurring because they are associated with high energy barriers. This problem can be solved either by performing long simulations exceeding time scales of conformational changes[5,19,20] or by free energy modeling.[21−29] In their seminal article, Biarnes and co-workers studied different ring conformations of β-D-glucopyranose by Car−Parrinello molecular dynamics simulation with a metadynamics bias potential.[21] They calculated the conformational free energy surface and identified the $^4C_1$ global free energy minimum and other boat/skew-boat local free energy minima.

Babin and Sagui used adaptively biased molecular dynamics (ABMD) and the Glycam 06 force field to predict the conformational free energy surface of methyl glycosides of α-L-iduronic acid and β-D-glucuronic acid (β-D-GlcA).[22] In agreement with experiments, they found that α-L-IdoA-OMe rather prefers the $^1C_4$ conformation, whereas, its C5-epimer β-D-GlcA-OMe significantly prefers the $^4C_1$ conformation.

Recently, Sattelle and co-workers exploited graphical processing units (GPUs) to perform an unbiased multimicrosecond molecular dynamics simulation of α-L-IdoA-OMe and the same molecule sulphated at 2-position, α-L-IdoA2S-OMe (Figure 1).[20] Both biased simulations of Babin and Sagui[22] and unbiased simulations of Sattelle and co-workers[20] are in good agreement and provide different views on the same system.

It has been recognized that scaling of noncovalent interactions between atoms separated by three covalent bonds (i.e., 1−4 interactions) play a crucial role in carbohydrate modeling. Kirschner and Woods performed molecular dynamics simulation of methyl glycosides of β-D-glucopyranose and β-D-galactopyranose in the Glycam 03 force field.[30] Resulting trajectories were analyzed to calculate the composition of rotamers of the hydroxymethyl group. They found that the scaling used for protein and nucleic acid modeling (van der Waals interactions divided by 2.0 and electrostatic interactions divided by 1.2) does not provide a reasonable rotamer composition. On the other hand, when these interactions were not scaled, the rotamer mixture was in excellent agreement with an experiment. This can be explained by the fact that scaling of 1−4 interactions perturbs the interplay between O-6···O-5 and O-6···O-4; the former being a 1−4 and the later being a 1−5 interaction. These results were confirmed by free energy modeling.[31]

Also the scaling of 1−4 interactions plays important role in modeling of ring conformations. It has been shown that conformational free energy surface of β-D-glucopyranose is more complicated when calculated with "protein" scaling compared to the free energy surface calculated without scaling.[23] The $^4C_1$ conformation is the global minimum for both scaling schemes, but the relative free energy of the $^1C_4$ significantly changes with scaling of 1−4 interactions.

In the above-mentioned study, Babin and Sagui[22] did not scale any 1−4 interactions. Sattelle and co-workers[20] also did not scale 1−4 electrostatic interactions, but 1−4 van der Waals interactions were scaled down by a factor of 2.0. This different setup is likely to cause minor, yet interesting, changes in the calculated equilibria of iduronic acid. The free energy of skew boat of α-L-IdoA-OMe was calculated by Babin and Sagui[22] to be between 12 and 13 kJ/mol (as deduced from Figure 3 in the Babin's article, relative to the $^1C_4$ conformation). This means that this conformation accounts for <1% of α-L-IdoA-OMe in solution. In contrast, it formed several percents of population in the trajectory calculated by Sattelle and co-workers.[20]

It is known that the ^2S_O conformation is a relevant conformation of iduronic acid. The free energy difference between all three conformations, $^1C_4$, $^4C_1$, and ^2S_O, is not likely to be high; otherwise, some of these conformations would become thermodynamically forbidden. For realistic modeling of glycoconjugates containing iduronic acid, it is necessary to use a molecular potential that accurately models the equilibrium of all three main conformers. The Glycam 06 with no scaling of electrostatic and van der Waals 1−4 interactions accurately models the equilibrium between both chairs, however, it disfavors the ^2S_O conformation. Scaling of van der Waals 1−4 interactions favors this conformation. Therefore, in this study we tested different scaling schemes of 1−4 interactions in free energy modeling of α-L-IdoA-OMe and α-L-IdoA2S-OMe. Metadynamics[32−34] with the bias potential acting in the space of three Cremer-Pople[35] puckering coordinates was used to improve sampling and to provide free energy estimates.

METHODS

All simulations were performed in Gromacs 4.0.7[36] with the modified Plumed 1.2.0[37] plug-in. The Glycam 06[38] was used as a force field. AMBER topology of α-L-IdoA2S-OMe was kindly provided by Dr. Benedict M. Sattelle.[20] Topologies were converted to Gromacs format by *amb2gmx.pl* script.[39] It was necessary to modify this script to avoid deletion of torsional terms with negative amplitudes as described elsewhere.[28] The molecule was placed to a 3 × 3 × 3 nm box. The box was then filled with an appropriate number of TIP3P water molecules and sodium counterions.

Electrostatic interactions were treated by particle-mesh Ewald methods[40] with a cutoff set to 1 nm. Temperature (300 K) was controlled using Berendsen thermostat.[41] After a short energy minimization (>10000 steepest-descent steps), the system was equilibrated by 500 ps unbiased simulation. This was followed by 10 ns metadynamics simulation. Time step was set to 1 fs, and no constraints were applied to the solute.

The Plumed plug-in was modified to allow for application of the Cartesian form of Cremer-Pople[35] coordinates (q_x, q_y, and q_z) instead of the polar form.[24] Cartesian Cremer-Pople coordinates are defined as

$$q_x = \sqrt{\frac{1}{3}} \sum_{j=1}^{6} z_j \cos\left[\frac{2\pi}{3}(j-1)\right]$$

$$q_y = \sqrt{\frac{1}{3}} \sum_{j=1}^{6} z_j \sin\left[\frac{2\pi}{3}(j-1)\right]$$

$$q_z = \sqrt{\frac{1}{6}} \sum_{j=1}^{6} (-1)^{(j-1)} z_j$$

where z_j is a displacement of a j-th atom from the plane of the ring. Width of each 3D Gaussian hill was 0.01 nm in all three directions, and height was 0.1 kJ/mol. The bias potential was added every 1000 steps (1 ps).

dx.doi.org/10.1021/jp3100552 | J. Phys. Chem. B 2013, 117, 1003−1009

The free energy surface is calculated as a negative value of metadynamics bias potential. The resulting 3D free energy surface was visualized using MayaVi2.[42] A free energy difference between two conformational families can be calculated as a difference of bias potentials in two points of the collective variable (CV) space, each point corresponding to each conformational family. A conformational family corresponding to a free energy minimum was identified from the value of the polar Cremer-Pople coordinate θ. At a certain stage of metadynamics when all major free energy minima had been flooded (in this work, it was between 7 and 10 ns, see Supporting Information) this difference is stable and fluctuates around an equilibrium free energy difference. This fluctuation was evaluated as a standard deviation, and its value describes convergence of sampling and accuracy of predicted equilibrium percentages. The equilibrium percentage of an i-th conformer was calculated as

$$p_i = 100\frac{\exp(-A_i/kT)}{\sum_j \exp(-A_j/kT)}$$

where A is the free energy and j goes over all free energy minima. Confidence intervals δp_i were calculated from free energies A and their standard deviations δA as

$$p_i + \Delta p_i = 100\frac{\exp(-A_{i,\min}/kT)}{\exp(-A_{i,\min}/kT) + \sum_{j\neq i} \exp(-A_{j,\max}/kT)}$$

$$p_i - \Delta p_i = 100\frac{\exp(-A_{i,\max}/kT)}{\exp(-A_{i,\max}/kT) + \sum_{j\neq i} \exp(-A_{j,\min}/kT)}$$

where $A_{i,\min}$ and $A_{i,\max}$ are equivalent to $A_i - \delta A_i$ and $A_i + \delta A_i$, respectively. Narrow confidence intervals demonstrate good convergence of metadynamics simulations.

Values of the $^3J_{H-C-C-H}$ were computed for six representative structures of each of four main minima ($^1C_4$, $^4C_1$, ^2S_O, and $^3S_1$) using Karplus-type equation developed by Hricovíni and Bízik.[43]

RESULTS

In this article, we use metadynamics simulation in explicitly modeled water with a bias potential acting in the space of three Cremer-Pople coordinates in order to evaluate how sensitive Glycam parametrization is to different 1−4 interaction scaling schemes, which have been recognized as an important factor in carbohydrate modeling.[30] Two different values of electrostatic scaling were tested, namely, 1.0 (no scaling) and 1.2 (a reduction of electrostatic interactions that is used in simulations of proteins, nucleic acids, and carbohydrate−protein complexes in force fields of the AMBER series). We tested four different van der Waals scaling schemes, the scaling factor of 1.0 (no scaling) and scaling factor 2.0 (standard AMBER scaling), as well as scaling by factors of 1.5 and 3.0, to estimate the trend in the observer effect. The simulations with scaling factors 1.5 and 3.0 were performed only with unscaled electrostatic interactions. In total, six different scaling schemes were tested for both α-L-IdoA-OMe and α-L-IdoA2S-OMe.

All simulations started from the $^4C_1$ conformation, and all relevant conformations were quickly sampled, owing to exceptional sampling efficiency of metadynamics. Examples of the resulting free energy surfaces are depicted in Figure 2 for

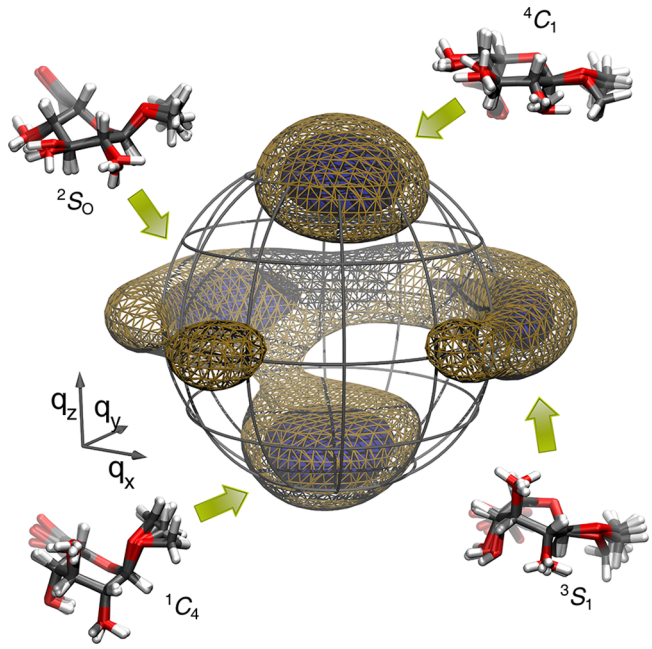

Figure 2. Conformational free energy surface of α-L-IdoA-OMe in the space of three Cremer-Pople coordinates depicted as isosurfaces at 20 kJ/mol (solid) and 30 kJ/mol (wireframe), both relative to the global minimum. Each principal free energy minimum is depicted as ten snapshots obtained from the metadynamics pseudotrajectory. Free energy surfaces were generated by MayaVi2.[42] Pictures of structures were generated by VMD[45] and PoVRay (http://www.povray.org).

scaling of 1−4 interactions down by the factor of 1.0 for electrostatics and 2.0 for van der Waals interactions. Three-dimensional free energy surfaces are depicted as isosurfaces at 20 (solid) and 30 kJ/mol (wireframe), which means that points inside "blobs" correspond to conformations with free energy lower than 20 and 30 kJ/mol, respectively, relative to the global minimum. Relative free energy values with confidence intervals are listed in Table 1. These values were used to predict relative conformer composition in equilibrium, which is depicted in Figure 3.

All simulations with scaling down of electrostatic 1−4 interactions by the factor of 1.2 predicted the $^4C_1$ conformation to be the global minimum, in contrast to the experimental results from the literature. Simulation without scaling of both electrostatic and van der Waals interactions modeled the $^1C_4$ conformation as the global minimum. The results for α-L-IdoA-OMe were in a good agreement with the simulation performed by Babin and Sagui, who used a different free energy modeling method called adaptively biased molecular dynamics simulation.[22]

Simulations with the scaling scheme used by Sattelle and co-workers,[20] that is, no scaling of electrostatic 1−4 interactions and scaling down of van der Waals interactions by the factor of 2.0 were not significantly different from the simulations where both electrostatic and van der Waals interactions were unscaled. A minor, yet significant, difference was observed in relative free energies of the ^2S_O conformation. This skew boat was virtually absent (<0.2%) when van der Waals interactions were unscaled. This agrees also with the simulation by Babin and Sagui.[22] However, the ^2S_O conformation formed 2.4 ± 1.4% in α-L-

dx.doi.org/10.1021/jp3100552 | J. Phys. Chem. B 2013, 117, 1003−1009

Table 1. Relative Free Energies (in kJ/mol) of Conformer Calculated by Different Scaling Schemes[a]

	Coul.	vdW	Coul.	vdW	Coul.	vdW	Coul.	vdW	Coul.	vdW	Coul.	vdW
scaling	1.2	1.0	1.2	2.0	1.0	1.0	1.0	1.5	1.0	2.0	1.0	3.0
conformation						α-L-IdoA-OMe						
$^1C_4$	0.0		0.0		0.0		0.0		0.0		0.0	
$^4C_1$	−31.8 ± 0.8		−32.0 ± 0.9		4.0 ± 1.6		4.7 ± 0.6		2.6 ± 1.1		2.8 ± 0.7	
^2S_O	−6.6 ± 0.7		−15.4 ± 0.9		17.9 ± 1.4		10.8 ± 0.8		8.5 ± 0.9		5.9 ± 0.8	
$^3S_1$	n.d.		−1.9 ± 0.9		18.4 ± 1.2		13.6 ± 0.5		12.1 ± 0.6		9.6 ± 0.7	
$^OS_2$	n.d.		n.d.		32.0 ± 1.1		27.5 ± 0.6		25.1 ± 1.3		23.2 ± 0.7	
$^1S_3$	11.0 ± 1.0		n.d.		34.9 ± 0.7		n.d.		n.d.		n.d.	
$^1S_5$	9.7 ± 1.4		5.2 ± 0.4		31.9 ± 0.8		26.7 ± 0.5		24.4 ± 1.8		27.1 ± 0.8	
$^5S_1$	n.d.		n.d.		25.2 ± 1.0		n.d.		n.d.		18.4 ± 1.0	
conformation						α-L-IdoA2S-OMe						
$^1C_4$	0.0		0.0		0.0		0.0		0.0		0.0	
$^4C_1$	−25.4 ± 1.4		−28.8 ± 0.6		10.4 ± 0.5		12.9 ± 1.3		13.3 ± 0.9		14.6 ± 1.1	
^2S_O	−6.4 ± 1.0		−18.5 ± 0.5		16.8 ± 0.9		14.1 ± 0.6		9.2 ± 0.7		6.6 ± 0.8	
$^3S_1$	n.d.		9.2 ± 1.3		17.3 ± 0.4		14.7 ± 0.4		10.8 ± 0.4		7.7 ± 0.5	
$^OS_2$	n.d.		n.d.		n.d.		n.d.		n.d.		n.d.	
$^1S_3$	n.d.		n.d.		n.d.		n.d.		n.d.		n.d.	
$^1S_5$	15.1 ± 0.6		5.8 ± 2.1		34.4 ± 0.7		32.1 ± 0.9		31.1 ± 0.5		29.7 ± 1.0	
$^5S_1$	n.d.		n.d.		n.d.		n.d.		26.2 ± 0.5		n.d.	

[a]Values are presented as mean ± s.d. (see Methods for details). Coul. = coulombic, vdW = van der Waals, n.d. = not determined.

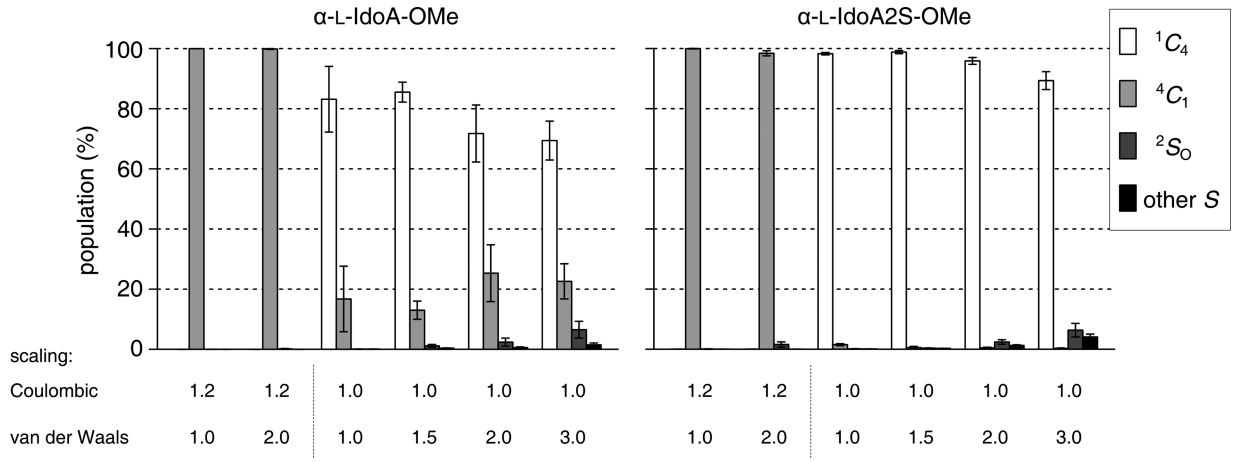

Figure 3. Predicted compositions of equilibrium mixtures. Error bars are calculated on the basis of standard deviations of relative free energy values, as described in Methods.

IdoA-OMe and 2.4 ± 0.9% in α-L-IdoA2S-OMe when van der Waals interactions were scaled down by the factor of 2.0. Sattelle and co-workers predicted higher value (approximately 7% for all nonchair structures), nevertheless, it is noteworthy that this trend was observed. Further scaling down of 1−4 van der Waals interactions tends to support this trend (Figure 3). Structures from all simulations were visually inspected to investigate whether high scaling of noncovalent interactions does not change the geometry in a nonrealistic way. Such distortions of structures were not observed.

Three conformations, $^1C_4$, $^4C_1$, and ^2S_O, were identified as minima of both carbohydrates and all simulation setups. The fourth minimum (referred to as "other *S*") was dependent on the carbohydrate molecule and setup. In most simulations, it was the $^3S_1$. This included simulations with the setup used by Sattelle and co-workers[20] and an agreement with their study was achieved. In simulations of α-L-IdoA-OMe with electrostatics scaling, the fourth minimum was the $^5S_1$. This minimum was also observed in all simulation, however, its free energy was high (>20 kJ/mol in simulations without scaling of electrostatic 1−4 interactions). Interestingly, all nonchair minima were skew-boats, no boats were observed as minima. It is appealing to look at transition states and underlying pathways of conformational changes. Figure 2 shows that the most favorable pathway of escape from the $^1C_4$ conformation was via ^2S_O. The free energy barrier of $^1C_4 \rightarrow {}^2S_O$ was approximately 29 and 27 kJ/mol for α-L-IdoA-OMe and α-L-IdoA2S-OMe, respectively, for the simulation without scaling of electrostatics and with van der Waals interactions scaled down by the factor of 2.0. This corresponds to transition half-times in tens of nanoseconds in agreement with unbiased simulations.[20]

The accuracy of the simulations with scaling of van der Waals interactions down by the factor of 2.0 (without scaling of Coulombic interactions) was evaluated by comparison of the computed values of three-bond proton−proton spin−spin coupling constants ($^3J_{H-C-C-H}$) with experimental data. Six representative conformations were selected for each of four minima ($^1C_4$, $^4C_1$, ^2S_O, and $^3S_1$) as conformations with minimal

dx.doi.org/10.1021/jp3100552 | J. Phys. Chem. B 2013, 117, 1003−1009

distances from the corresponding free energy minimum. Values of the $^3J_{H-C-C-H}$ were then calculated as population-averaged values across all minima. The results (see Supporting Information) were in agreement with the study of Sattelle and co-workers.[20] Values of $^3J_{H-C-C-H}$ were slightly lower than experimental values, similarly to the study of Sattelle and co-workers; nevertheless, the observed trend was very similar.

The strong influence of 1−4 electrostatic interactions scaling can be explained by the presence of repulsive interactions between oxygen atoms of hydroxyl groups. These atoms are in a relative 1−4 arrangement, that is, O-1 with O-2, O-2 with O-3, and O-3 with O-4. In the $^4C_1$ conformation, these atoms are in a relative *gauche* orientation, with a distance between neighboring oxygen atoms ranging between 2.7 and 3.0 Å. On the other hand, this orientation changes to *trans* in the $^1C_4$ conformation. Simultaneously, distance between neighboring oxygen atoms rises to approximately 3.6−3.8 Å. Scaling (reduction) of these repulsive interactions favors the conformation with lower O···O distance, which is the $^4C_1$ conformation. This effect has been observed in β-D-glucopyranose, where the absence of scaling stabilized the $^1C_4$ conformation by 34 kJ/mol, but still not enough to become the global minimum.[23] The stabilization effect in α-L-IdoA-OMe was similar (approximately 36 kJ/mol). In contrast to β-D-glucopyranose, the scaling changes the order of both chair conformations. The $^4C_1$ conformation was modeled as the global minimum of α-L-IdoA-OMe when electrostatic interactions were scaled down, whereas the $^1C_4$ conformation was modeled as the global minimum in simulation without scaling of 1−4 electrostatics. It must be said that also other factors and interactions may play a role, beside repulsive O···O interactions.

The effect of van der Waals 1−4 interactions is more difficult to explain. Scaling of these interactions does not significantly perturb the equilibrium between conformations $^1C_4$ and $^4C_1$, but it stabilizes the ^2S_O conformation. One possible explanation is that boat and skew-boat conformations contain dihedral angles with values different from "canonical" values of approximately 60, 180, and 300°. A structure with a dihedral angle lower than 60° is characterized by a shorter distance between atoms in 1−4 relative position. Therefore, van der Waals repulsion between these atoms is reduced in the simulation scheme with scaling of 1−4 van der Waals interactions. Examples of such dihedrals are C-3−C-4−C-5−O-5 (approximately +30°) and O-5−C-1−C-2−C-3 (approximately +20°) in the ^2S_O conformation. However, also other factors can play a role in the effect of scaling of 1−4 van der Waals interactions, similar to the effect of scaling of electrostatic 1−4 interactions.

The effect proposed in previous paragraphs can be illustrated by detailed analysis, as presented in Figure 4. Each conformational family is represented by five snapshots selected from the simulation of α-L-IdoA-OMe (scaling of van der Waals interactions down by 2.0 and no scaling of electrostatics). Potential energies of selected 1−4 pairs were calculated using force field parameters. Electrostatic interactions were calculated by Coulomb's law in vacuum and without taking the periodicity into the account. Both electrostatic and van der Waals interactions are depicted as unscaled values. All tested 1−4 interactions were repulsive.

Figure 4A shows electrostatic interactions between exocyclic oxygen atoms. Energies of interaction between O-1 and O-2 atoms were similar for all conformations. This can be explained by the fact that the α-anomer was studied. On the other hand,

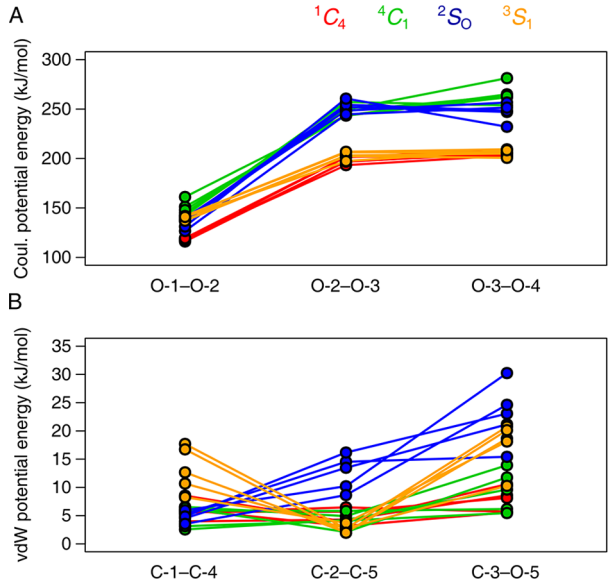

Figure 4. Potential energies of noncovalent 1−4 interactions of selected atom pairs in different conformational families. Values are depicted in the unscaled form (see Results for details). Each conformational family was represented by five snapshots from metadynamics simulation of α-L-IdoA-OMe (scaling of van der Waals interactions down by 2.0 and no scaling of electrostatics).

O-2−O-3 and O-3−O-4 interactions were more repulsive (by approximately 50 kJ/mol) for $^4C_1$ and ^2S_O, compared to $^1C_4$ and $^3S_1$. This makes a difference of approximately 10 kJ/mol between scaling factors 1.2 and 1.0. This explains the fact that a simulation with electrostatic interactions scaled by the factor 1.2 prefers $^4C_1$, whereas a simulation without scaling prefers the $^1C_4$ conformation.

Energies of van der Waals 1−4 interactions between ring atoms are shown in Figure 4B. Values for $^1C_4$ and $^4C_1$ conformations were low, ranging from 0 to +10 kJ/mol. On the other hand, for skew-boats there was at least one 1−4 pair with high values of van der Waals interactions. Namely, C-2−C-5 with C-3−O-5 interactions destabilize $^2S_0$ and C-1−C-4 with C-3−O-5 destabilize the $^3S_1$ conformation. This explains why scaling of 1−4 van der Waals interactions promotes the formation of the boat and skew-boat conformations.

It is also necessary to check whether the change in scaling of van der Waals 1−4 interactions does not alter the performance of the studied force field in modeling of other systems and other degrees of freedom. The setup with scaling of van der Waals 1−4 interactions down by the factor of 2.0 was tested on conformational equilibria of β-D-Glc-OMe. The $^4C_1$ conformation was modeled as the global free energy minimum. The second and third most stable conformations were $^1C_4$ and boats/skew-boats, both at approximately 15 kJ/mol. The $^1S_3$ was the preferred conformation among boats/skew-boats. This clearly shows that the $^4C_1$ conformation accounts for ∼99.5% and $^1C_4$ with boats/skew-boats both account for ∼0.2% (see Supporting Information), in agreement with experimental results.

We also repeated the calculation of conformational equilibria of rotamers of C-5−C-6 bond in α-D-Glc-OMe and α-D-Gal-OMe.[28] van der Waals 1−4 interactions were scaled down by the factor of 2.0. The resulting conformational free energy surface has shown relatively low free energy differences similarly to simulations without scaling.[28] For α-D-Glc-OMe,

dx.doi.org/10.1021/jp3100552 | J. Phys. Chem. B 2013, 117, 1003−1009

the populations were calculated as 58, 41 and 2%, for *gg*, *gt*, and *tg*, respectively. Values calculated without scaling[28] were 63, 36, and 1%. The results for α-D-Gal-OMe were 5, 75, and 19%, for *gg*, *gt*, and *tg*, respectively, compared to 5, 83, and 12% without scaling.[28] These results show that scaling of van der Waals 1−4 interactions does not significantly disturb equilibria of rotamers of a hydroxymethyl group (see Supporting Information).

DISCUSSION

In past, carbohydrate force fields were designed to keep rigid chair conformations of basic pyranose sugars during the time course of molecular simulations of glycoconjugates and their complexes. The situation is different for iduronic acid because this residue is far from rigid. Prediction of structures, equilibria and dynamics of glycoconjugates containing these residues is more difficult task. Modeling of conformational equilibria in pyranose sugars is relatively sensitive to small changes in the potential energy function. This is especially true for iduronic acid and its derivatives because all three forms of this sugar can coexist in equilibrium mixture. It must be kept in mind that 1 kJ/mol change of relative free energy cause a population reduction/enrichment in tens of percent. Nevertheless, several studies indicate[20,22] that the Glycam force field models this equilibrium with high accuracy. This has been confirmed also by this study.

We have shown that not only scaling of electrostatics, but also scaling of van der Waals interaction can tune performance of molecular mechanics force fields in modeling of pyranose puckering. The question arises whether this modification should be adopted by the community for modeling of carbohydrates. As already mentioned, most other monosaccharides are rigid, and changes in van der Waals scaling are not likely to introduce any significant change in its conformational preferences. Moreover, the Glycam force field is designed to be general. This means that it is suitable not only for pure carbohydrates, but also to be easily customizable for carbohydrate-like molecules. For these reasons, it does not seem to be useful to modify the Glycam force field by changing the van der Waals scaling parameters. On the other hand, this modification can be useful in simulations of systems containing iduronic acid, both biased and unbiased, when determination of accurate composition of different puckering forms is wanted. This is particularly relevant in simulations aimed at the determination of how the conformational behavior of iduronic acid is influenced by its modifications, by the context of oligosaccharide structure or noncovalent interaction with other binding partners.

The gauche effect is a fundamental phenomenon shaping structures of carbohydrate molecules.[44] It is defined as a tendency of O−C−C−O moiety (alternatively oxygen can be replaced by other electronegative atom) to adopt the *gauche* conformation in contrast to the situation in C−C−C−C where *trans* conformation is typical. Based on these results, it can be said that scaling of 1−4 electrostatics supports the gauche effect in the context of the studied molecule.

In conclusion, the results indicate that scaling of 1−4 interactions can be used to control the performance of carbohydrate force fields in modeling of pyranose puckering. This situation is similar to modeling of rotamer equilibria of hydroxymethyl moiety in β-D-glucopyranose-OMe and β-D-galactopyranose-OMe.[30,31] Similar to this classical system of carbohydrate chemistry, the conformational equilibria of ring puckering can be "tuned" by scaling of noncovalent 1−4 interactions. Data obtained with van der Waals 1−4 interactions scaled down by the factor of 2.0 and without scaling of Coulombic interactions were in good agreement with results of unbiased simulation of Sattelle and co-workers[20] and with experimental data published therein.

ASSOCIATED CONTENT

Supporting Information

Time development of collective variables during metadynamics simulations, comparison with experimental data and metadynamics simulations of α-D-Glc-OMe and α-D-Glc-OMe are presented. This material is available free of charge via the Internet at http://pubs.acs.org.

AUTHOR INFORMATION

Corresponding Author

*E-mail: spiwokv@vscht.cz. Fax: +420 220 445 167. Tel.: +420 220 443 028.

Notes

The authors declare no competing financial interest.

ACKNOWLEDGMENTS

This work was supported by the Czech Ministry of Education, Youth and Sports (MSM6046137305), seventh FP EU (NMP4-LA-2008-212043), and the Scientific Grant Agency of the Ministry of Education of Slovak Republic and the Slovak Academy of Sciences (VEGA-02/0176/09). The access to the National Grid Infrastructure MetaCentrum ("Projects of Large Infrastructure for Research, Development, and Innovation", LM2010005) and the Centre CERIT Scientific Cloud (part of Operational Program Research and Development for Innovations, Reg. No. CZ. 1.05/3.2.00/08.0144) is highly appreciated. Authors would like to thank Dr. Benedict M. Sattelle for force field parameters of α-L-IdoA2S-OMe.

REFERENCES

(1) Brooks, S. A.; Dwek, M. V.; Schumacher, U. *Functional and Molecular Glycobiology*; BIOS: Oxford, 2002.
(2) Casu, B.; Petitou, M.; Provasoli, M.; Sinaÿ, P. *Trends Biochem. Sci.* **1988**, *13*, 221−225.
(3) Ochsenbein, P.; Bonin, M.; Schenk-Joss, K.; El-Hajji, M. *Angew. Chem., Int. Ed.* **2011**, *50*, 11637−11639.
(4) Rudd, T. R.; Skidmore, M. A.; Guerrini, M.; Hricovíni, M.; Powell, A. K.; Siligardi, G.; Yates, E. A. *Curr. Opin. Struct. Biol.* **2010**, *20*, 567−574.
(5) Sattelle, B. M.; Almond, A. *Glycobiology* **2011**, *21*, 1651−1662.
(6) Sattelle, B. M.; Almond, A. *Phys. Chem. Chem. Phys.* **2012**, *14*, 5843−5848.
(7) Sattelle, B. M.; Bose-Basu, B.; Tessier, M.; Woods, R. J.; Serianni, A. S.; Almond, A. *J. Phys. Chem. B* **2012**, *116*, 6380−6386.
(8) Davies, G. J.; Planas, A.; Rovira, C. *Acc. Chem. Res.* **2012**, *45*, 308−316.
(9) Marszalek, P.; Oberhauser, A.; Pang, Y.; Fernandez, J. *Nature* **1998**, *396*, 661−664.
(10) Nieto, L.; Canales, Á.; Giménez-Gallego, G.; Nieto, P. M.; Jiménez-Barbero, J. *Chem.—Eur. J.* **2011**, *17*, 11204−11209.
(11) García-Mayoural, M. F.; Canales, Á.; Díaz, D.; López-Prados, J.; Moussaoui, M.; de Paz, J. L.; Angulo, J.; Nieto, P. M.; Jiménez-Barbero, J.; Boix, E.; Bruix, M. *ACS Chem. Biol.* **2012**, DOI: 10.1021/cb300386v.
(12) Hricovíni, M. *J. Phys. Chem. B* **2011**, *115*, 1503−1511.
(13) Jin, L.; Hricovíni, M.; Deakin, J. A.; Lyon, M.; Uhrin, D. *Glycobiology* **2009**, *19*, 1185−1196.
(14) Hricovíni, M.; Scholtzová, E.; Bízik, F. *Carbohydr. Res.* **2007**, *342*, 1350−1356.

(15) Hricovíni, M. *Carbohydr. Res.* **2006**, *341*, 2575−2580.
(16) Remko, M.; von der Lieth, C. *J. Chem. Inf. Model.* **2006**, *46*, 1194−1200.
(17) Kurihara, Y.; Ueda, K. *Carbohydr. Res.* **2006**, *341*, 2565−2574.
(18) Taylor, C. J.; Nix, M. G. D.; Dessent, C. E. H. *J. Phys. Chem. A* **2010**, *114*, 11153−11160.
(19) Gandhi, N. S.; Mancera, R. L. *Carbohydr. Res.* **2010**, *345*, 689−695.
(20) Sattelle, B. M.; Hansen, S. U.; Gardiner, J.; Almond, A. *J. Am. Chem. Soc.* **2010**, *132*, 13132−13134.
(21) Biarnés, X.; Ardevol, A.; Planas, A.; Rovira, C.; Laio, A.; Parrinello, M. *J. Am. Chem. Soc.* **2007**, *129*, 10686−10693.
(22) Babin, V.; Sagui, C. *J. Chem. Phys.* **2010**, *132*, 104108.
(23) Spiwok, V.; Králová, B.; Tvaroška, I. *Carbohydr. Res.* **2010**, *345*, 530−537.
(24) Autieri, E.; Sega, M.; Pederiva, F.; Guella, G. *J. Chem. Phys.* **2010**, *133*, 095104.
(25) Kuttel, M. M. *Mini-Rev. Org. Chem.* **2011**, *8*, 256−262.
(26) Hansen, H. S.; Hünenberger, P. H. *J. Comput. Chem.* **2011**, *32*, 998−1032.
(27) Barnett, C. B.; Naidoo, K. J. *Mol. Phys.* **2009**, *107*, 1243−1250.
(28) Spiwok, V.; Tvaroška, I. *J. Phys. Chem. B* **2009**, *113*, 9589−9594.
(29) Soliman, M. E. S.; Pernia, J. J. R.; Greig, I. R.; Williams, I. H. *Org. Biomol. Chem.* **2009**, *7*, 5236−5244.
(30) Kirschner, K.; Woods, R. *Proc. Natl. Acad. Sci. U.S.A.* **2001**, *98*, 10541−10545.
(31) Spiwok, V.; Tvaroška, I. *Carbohydr. Res.* **2009**, *344*, 1575−1581.
(32) Laio, A.; Parrinello, M. *Proc. Natl. Acad. Sci. U.S.A.* **2002**, *99*, 12562−12566.
(33) Laio, A.; Gervasio, F. L. *Rep. Prog. Phys.* **2008**, *71*, 126601.
(34) Barducci, A.; Bonomi, M.; Parrinello, M. *WIRES: Comput. Mol. Sci.* **2011**, *1*, 826−843.
(35) Cremer, D.; Pople, J. *J. Am. Chem. Soc.* **1975**, *97*, 1354−1358.
(36) Hess, B.; Kutzner, C.; van der Spoel, D.; Lindahl, E. *J. Chem. Theory Comput.* **2008**, *4*, 435−447.
(37) Bonomi, M.; Branduardi, D.; Bussi, G.; Camilloni, C.; Provasi, D.; Raiteri, P.; Donadio, D.; Marinelli, F.; Pietrucci, F.; Broglia, R. A.; Parrinello, M. *Comput. Phys. Commun.* **2009**, *180*, 1961−1972.
(38) Kirschner, K. N.; Yongye, A. B.; Tschampel, S. M.; Gonzalez-Outeirino, J.; Daniels, C. R.; Foley, B. L.; Woods, R. J. *J. Comput. Chem.* **2008**, *29*, 622−655.
(39) Sorin, E.; Pande, V. *Biophys. J.* **2005**, *88*, 2472−2493.
(40) Essmann, U.; Perera, L.; Berkowitz, M.; Darden, T.; Lee, H.; Pedersen, L. *J. Chem. Phys.* **1995**, *103*, 8577−8593.
(41) Berendsen, H.; Postma, J.; van Gunsteren, W.; di Nola, A.; Haak, J. *J. Chem. Phys.* **1984**, *81*, 3684−3690.
(42) Ramachandran, P.; Varoquaux, G. *IEEE Comput. Sci. Eng.* **2011**, *13*, 40−51.
(43) Hricovíny, M.; Bízik, F. *Carbohydr. Res.* **2007**, *342*, 779−783.
(44) Tvaroška, I.; Carver, J. *J. Phys. Chem. B* **1997**, *101*, 2992−2999.
(45) Humphrey, W.; Dalke, A.; Schulten, K. *J. Mol. Graph.* **1996**, *14*, 33−38.